NDE Technologies for Ceramic Matrix Composites: Oxide and Non-Oxide

J. G. Sun, C. M. Deemer, W. A. Ellingson, and J. Wheeler
Energy Technology Division
Argonne National Laboratory
9700 South Cass Avenue
Argonne, IL 60439

Abstract
Ceramic matrix composites (CMCs) usually are classified into two materials systems: oxide-based and non-oxide-based. Oxide-based systems consist of an oxide fiber and an oxide matrix, whereas non-oxide systems can consist of carbon fibers with a carbon matrix (Carbon/Carbon), carbon fibers with a silicon carbide matrix (Carbon/SiC), as well as silicon carbide fibers with a silicon carbide matrix (SiC/SiC). In addition, several processing methods affect the mechanical and thermal properties of these materials and thus affect the nondestructive evaluation (NDE) applications. Furthermore, most of these materials utilize an environmental barrier coating that protects the base material. This added layer also complicates the NDE applications. NDE technologies have been developed for characterizing these advanced material systems during manufacture so that process improvements can be assessed, and for "health" monitoring during service. Also, initial work has been done to estimate "remaining" useful life. NDE technologies that have been demonstrated to be applicable include thermal imaging that uses high-frame-rate, focal–plane-array infrared imagers with special software; air-coupled ultrasonics in through-transmission mode; X-ray computed tomographic imaging with large-area, small-pixel-size detectors; guided plate waves; and impact excitation resonance to measure internal friction. This paper discusses these NDE technologies and the protocols to be used for these materials.

1.0   Introduction

Ceramic matrix composite (CMC) materials are currently being developed for various high-temperature commercial and military applications, including advanced gas turbine engines. The extensive use of CMC materials is due to their relatively high strength/toughness and resistance to chemical reactions at high temperatures and their relatively low density [Evans and Naslain, 1995a-b].

CMCs are usually classified into two materials systems: oxide-based and non-oxide-based. Oxide-based CMCs consist of an oxide fiber and an oxide matrix such as Al_2O_3/Al_2O_3, whereas non-oxides can consist of carbon fibers with a carbon matrix (C/C), carbon fibers with a silicon carbide matrix (C/SiC), as well as silicon carbide fibers with a silicon carbide matrix (SiC/SiC). CMC materials are fabricated by several processing methods, which determine their mechanical and thermal properties. The fiber architectures of these composites varies and maybe planar (one-dimensional [1D]), as well as two- or three-dimensional (2-D or 3-D) [Ko, 1989]. The fiber structures can be densified with the matrix material by using various processes such as polymer impregnation and pyrolysis (PIP), chemical vapor infiltration (CVI), melt infiltration (MI), and sol-gel processing. Because of the complex microstructures and multiple processing steps involved during their fabrication, CMC components may contain flaws or defects of various sizes and shapes. Most of the large discrete defects are in the forms of delaminations and

large voids that are due to processing upset or service damage. However, CMCs may also contain a large number of microscopic flaws such as interface cracks, and cracks and porosities within the matrix. These small flaws, when combined with a compilation of damage modes, including environmental degradation, dynamic mechanical loading, and temperature fluctuations, may eventually cause the component to fail. In addition, CMC components utilized in gas engines are typically coated on the hot surfaces by an environmental barrier coating (EBC) to protect the CMCs from oxidation damage [Price et al., 2000; Miriyala et al., 2001; Eaton et al., 2001]. Erosion of the EBC layer and debonding between the EBC and CMC are major concerns of these material systems.

To reduce the likelihood of costly shut downs caused by failure of a CMC component in an engine, the component must be inspected for flaws and defects before it goes into service. This inspection is critical to determine the performance and reliability of the component. In most instances, because the cost associated with CMC fabrication is high, the testing must be nondestructive [Ellingson and Deemer, 2004]. To meet this need, we developed several nondestructive evaluation (NDE) technologies for characterizing advanced material systems during manufacture so process improvements can be assessed, and for "health" monitoring during service. Also, initial work has been done to estimate "remaining" useful life. NDE technologies that have been demonstrated to be applicable for CMC characterization include thermal imaging that uses high-frame-rate, focal–plane-array infrared imagers with special software; air-coupled ultrasonics in through-transmission mode; X-ray computed tomographic (CT) imaging with large-area, small-pixel-size detectors; guided plate waves; and impact excitation resonance to measure internal friction. Most of these NDE technologies are noncontact and produce image data [Ellingson and Deemer, 2002].

2.0   Description of NDE technologies

2.1   Thermal imaging

Thermal imaging relies on generating and monitoring a transient heat transfer process to determine the thermal property or thickness of a specimen. Figure 1a shows a typical experimental system in a through-transmission configuration. The apparatus includes an high-speed infrared (IR) camera that consists of a focal-plane array of IR detectors, a Pentium-based PC equipped with a digital frame grabber, a flash lamp unit for the thermal impulse, a function generator to provide an adjustable frame rate for the camera, and a dual-timing trigger to simultaneously trigger the flash lamps and data acquisition. An analog video system is used to monitor the experiments. During an experiment, the flash lamps provide an initial thermal impulse on the specimen and the resultant thermal response is measured by the IR camera and recorded to a computer for further analysis. The system operates in two modes: through-transmission, where the flash lamps and the IR camera are facing opposite surfaces of the specimen; and single-sided, where the flash lamps and the IR camera are on the same side of the specimen. The through-transmission setup is mostly used for mapping thermal diffusivity; the one-sided setup for measuring delamination depth.
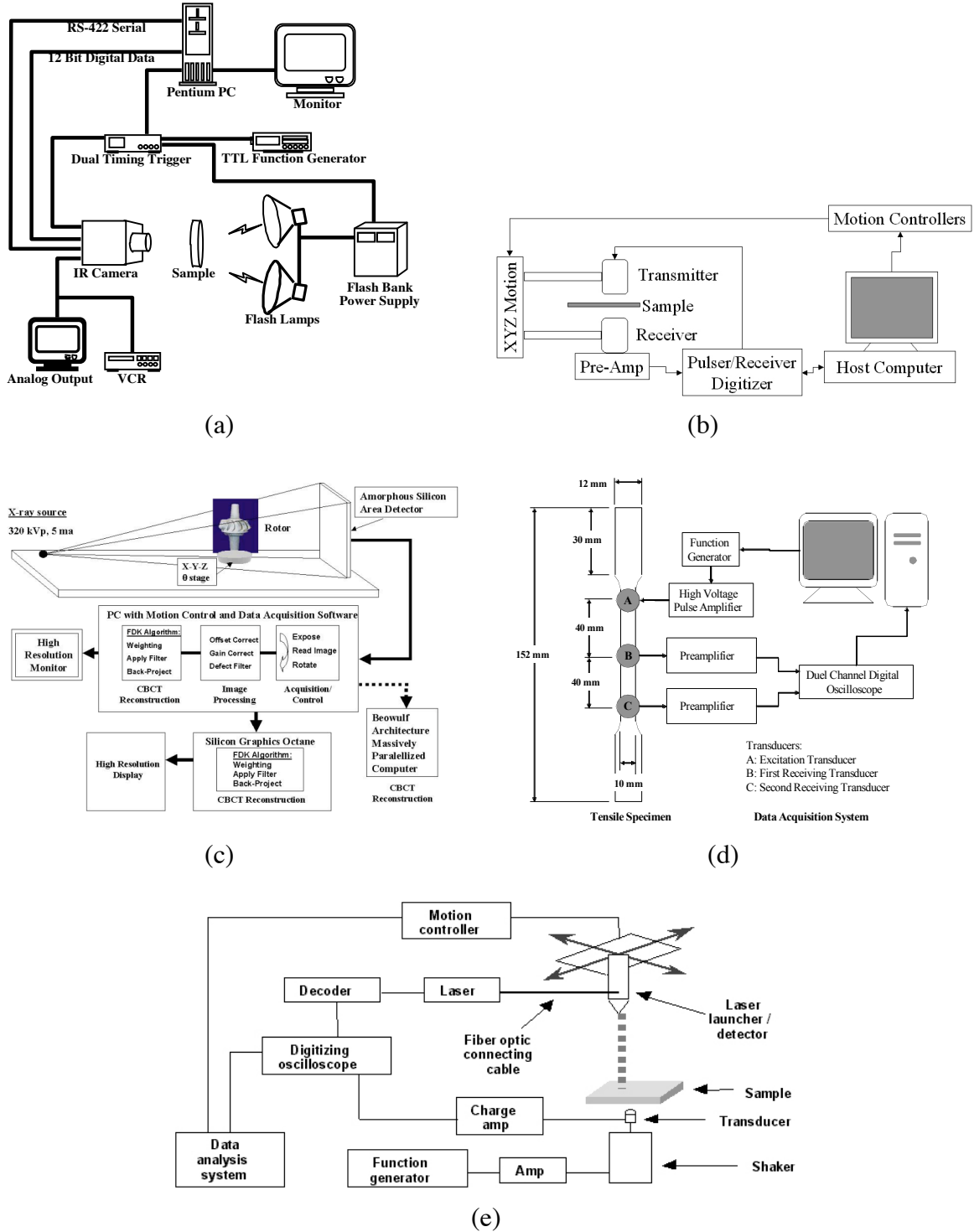
(a)

(b)

(c)

(d)

(e)

Fig. 1.　Schematic diagram of　(a) thermal imaging apparatus, (b) air-coupled ultrasonic system, (c) X-ray CT system, (d) guided-plate-wave system, and (e) impact acoustic resonance system.

2.1.1   Through-thickness thermal diffusivity mapping

Through-transmission pulsed thermal imaging has been used to determine full-field, through-thickness thermal diffusivity distributions [Stuckey et al., 1998; Sun et al., 1999]. In this method, the back surface of a sample is heated by an instantaneous thermal impulse. The rate of heat conduction through the thickness is directly related to the thermal diffusivity. The front-surface temperature rises as a function of time, following the theory of Parker et al. [1961]. The surface temperature curve, which can be measured by an IR camera, can serve as the basis for several methods that are used to calculate diffusivity. The simplest, and most efficient, method is to determine the characteristic "half-rise" time $t_{1/2}$, which represents the time when the front-surface temperature rises to one half of the maximum temperature increase. The through-thickness thermal diffusivity α is then calculated from

$$\alpha = \frac{0.139L^2}{t_{1/2}},$$

where L is the sample thickness. The accuracy of this method was calibrated with a NIST standard graphite specimen. Measured diffusivity was within 3% of the reported diffusivity of the material [Stuckey et al., 1998].

2.1.2   One-sided measurement of delamination depth

One-sided pulsed thermal imaging can be used to determine the size and depth of delaminations. After the flash heating, the decay rate of surface temperature depends on the heat flux within the specimen. When the heat flux reaches a delamination, which is filled by air with higher thermal resistance, the heat transfer rate is reduced in the region above the delamination. The surface above this region will show as a local "hot spot" at a higher temperature than the surrounding areas. The hot spot appears earlier during the transient if the delamination is shallow and later if the delamination is deep. A theoretical model has been developed to represent this heat transfer process. The defect depth or sample thickness (in the sound-material region) can be determined [Sun, 2003] by fitting the theoretical model with measured temperature data.

2.2   Through-transmission air-coupled ultrasonics

The air-coupled ultrasonic method, a relatively new method, was introduced in 1995. The method has become feasible primarily through advances in piezo-electrics and digital signal processing. It is especially beneficial to CMC materials because CMCs can be sensitive to moisture if tested in conventional water-coupled systems. A typical air-coupled, through-transmission system [Pillai et al., 1997] consists of a traditional computer-controlled x-y-z positioning system with two matched piezo-electric air-coupled transducers, as shown in Fig. 1b. Tone bursts of acoustic energy at 0.4 MHz from the emitting transducer are incident on the sample, without any immersion fluid or special coupling. The transmitted energy is detected by the receiving transducer, which contains a very-low-noise high-gain preamplifier. The detected signal from the preamplifier is used as input to a highly tuned amplifier and to an electronic time gate. The digital value of the peak voltage in a preset time gate is displayed and plotted in an x-y

array. An "image," referred to as a C-scan image, of the component under study is built up in both x and y directions. Attenuation of the acoustic signal is caused by differences in the material, e.g., a delamination, change in density, etc.

2.3   X-ray computed tomography

While conventional X-ray through-transmission imaging may be useful for simple flat plates, density mapping of more complex objects requires the use of CT imaging. In this method, see Fig. 1c, an X-ray source is coupled with a 2-D (or area) X-ray detector. The output of the detector is coupled directly to a powerful PC or workstation that contains image-processing software. The specimen under study is placed on a computer-controlled rotating table between the X-ray source and the detector. In this case, it is necessary to obtain a sequence of projection images with the computer-controlled table. The set of images (or X-ray attenuation data) is then used to "reconstruct" cross sections of the specimen. Because the reconstructed image is obtained from measurements of the relative X-ray attenuation, the image gray tones, if properly obtained, can be correlated to density, and, because a 3-D image can be obtained, the density can be determined in three dimensions.

2.4   Guided plate waves

Recent work [Deemer, 2003; Morscher, 1999] has shown that guided plate waves can be used to measure in-plane elastic modulus and that this can track damage states. The experimental setup for guided-plate-wave measurement is shown in Fig. 1d; three acoustic-emission transducers are used, each with a 150-kHz center frequency. One transducer is used to generate an acoustic pulse and two other transducers, with a well-defined separation distance, are used to measure the time of flight (TOF) of the elastic wave. This TOF measurement can be used to determine the elastic modulus, which, in turn, can be related to a damage parameter D [Krajcinovic, 1984] as

$$D = 1 - \frac{E}{E_o},$$

where E is the measured elastic modulus after the material has been subjected to various load conditions, and E_o is the elastic modulus of the new material before any exposure to loads.

2.5   Impact acoustic resonance

Impact acoustic resonant spectroscopy, often referred to as the "ping" test, is a method commonly used to determine damping behavior and resonant frequencies of a component. These properties are especially important for rotating components in turbomachinery. Figure 1e shows a schematic diagram of a typical system. The impact is applied by a controlled electro-dynamic shaker with an instrumented "impact" hammer. A noncontact laser vibrometer is used to detect the vibrational displacement, or a capacitance microphone is used to detect sound. Both of the analog signals are digitized in a high-frequency digitizer and the resultant signals are analyzed by frequency analysis software packages to determine the resonant frequency peaks and the specific damping capacity of the specimen. The damping capacity and peak amplitude can be correlated to the porosity of the entire component.

3.0 NDE Applications for CMCs

3.1 Density/porosity measurement

Density/porosity is an important parameter for CMC materials because it is related to the uniformity and completeness of the material processing. Three primary NDE methods can be used to measure density/porosity: thermal imaging, air-coupled ultrasonics, and X-ray CT. Through-thickness thermal imaging directly measures thermal diffusivity, which is a function of density. Figure 2a shows measured thermal diffusivity/mass density relationships for SiC/SiC standards [Sun et al., 1999]. Density is also related to ultrasonic attenuation [Sun et al., 1998a] and X-ray attenuation. These methods are also capable of determining spatial variation in density. One test sample [Ellingson et al., 2000], a melt-infiltrated SiC/SiC cylinder for a gas turbine combustor liner, had experienced an "upset" during processing (insufficient infiltration). NDE data, shown in Figs. 2b and 2c, suggested that there was a clearly detectable difference at the process-upset position. Subsequent destructive analysis, as noted in Fig. 2d, detected a difference in porosity.
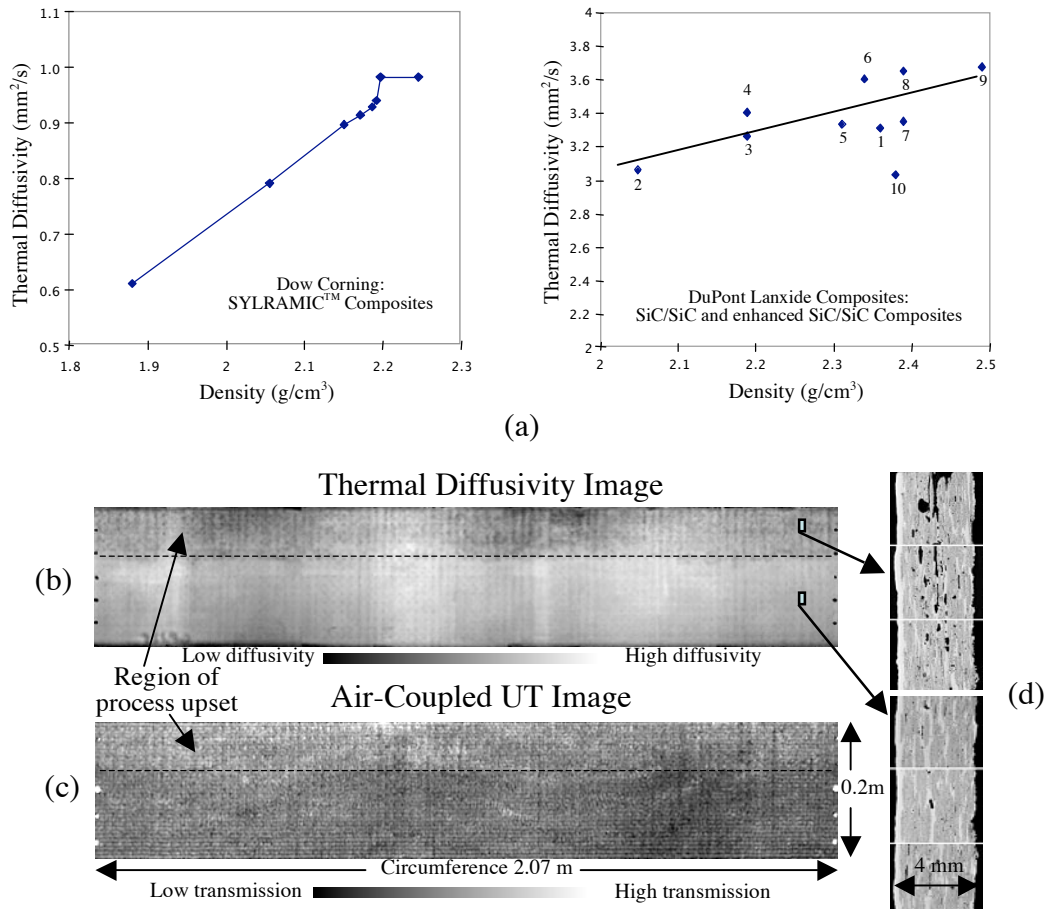

(a)

Fig. 2. (a) Thermal diffusivity as a function of density/porosity, and detection of porosity in MI SiC/SiC: (b) through-thickness thermal diffusivity data, (c) air-coupled ultrasonic through-transmission data, (d) destructive verification of porosity variation.

3.2   Material processing and damage repair

Thermal imaging and air-coupled ultrasound were used to investigate flat CMC panels during PIP processing cycles [Sun et al., 1998a]. The test samples for these experiments were 8-ply cloth in a 2-D lay-up. Because the PIP process allows sample removal between successive processing cycles, the same panels were examined by NDE methods after 1, 5, 10 and 15 cycles. Results of thermal diffusivity imaging of the 8-ply panel are shown in Figs. 3a-d. This series of images shows the diffusivity increase (lighter grayscale) due to increased density in the panel, and in addition, it shows the progressive repair of initially delaminated (dark) regions. After one PIP cycle, two large delaminated regions were noted in the upper left and upper right corners. Visual inspection of the edge revealed ply separation. After 5 cycles, handling damage enlarged some of the delaminated regions but also noted was some infiltration into the delaminated regions; this infiltration acted as a form of repair. Additional filling of the delaminated regions was detected after 10 cycles. Figures 3d and 3e show both thermal diffusivity image data and air-coupled ultrasonic data for the 8-ply lay-up samples after 15 PIP cycles. The correlation between the thermal image data and the air-coupled ultrasonic data is apparent.
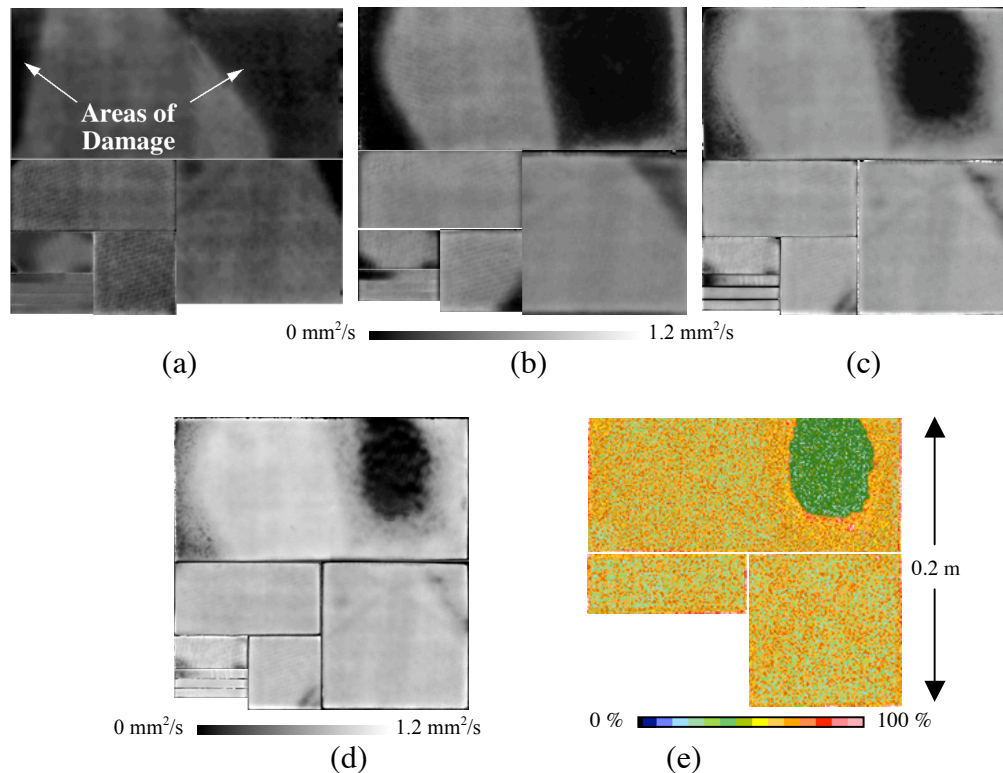

Fig. 3.   NDE data of 8-ply SYLRAMIC™ composite panel: thermal diffusivity images obtained after (a) 1, (b) 5, (c) 10, and (d) 15 PIP cycles and (e) air-coupled UT transmission images after 15 PIP cycles.

3.3 Thermal shock damage

Thermal shock damage in CVI SiC/SiC coupons was examined by the thermal diffusivity imaging method [Wang et al., 1998]. These coupons were quenched in water with quenching temperature differences ΔT up to 1000°C. Figure 4a shows diffusivity images of a coupon before and after quenching with ΔT = 1000°C. The thermal shock damage, represented by reduced thermal diffusivity, was severe at the coupon edges.
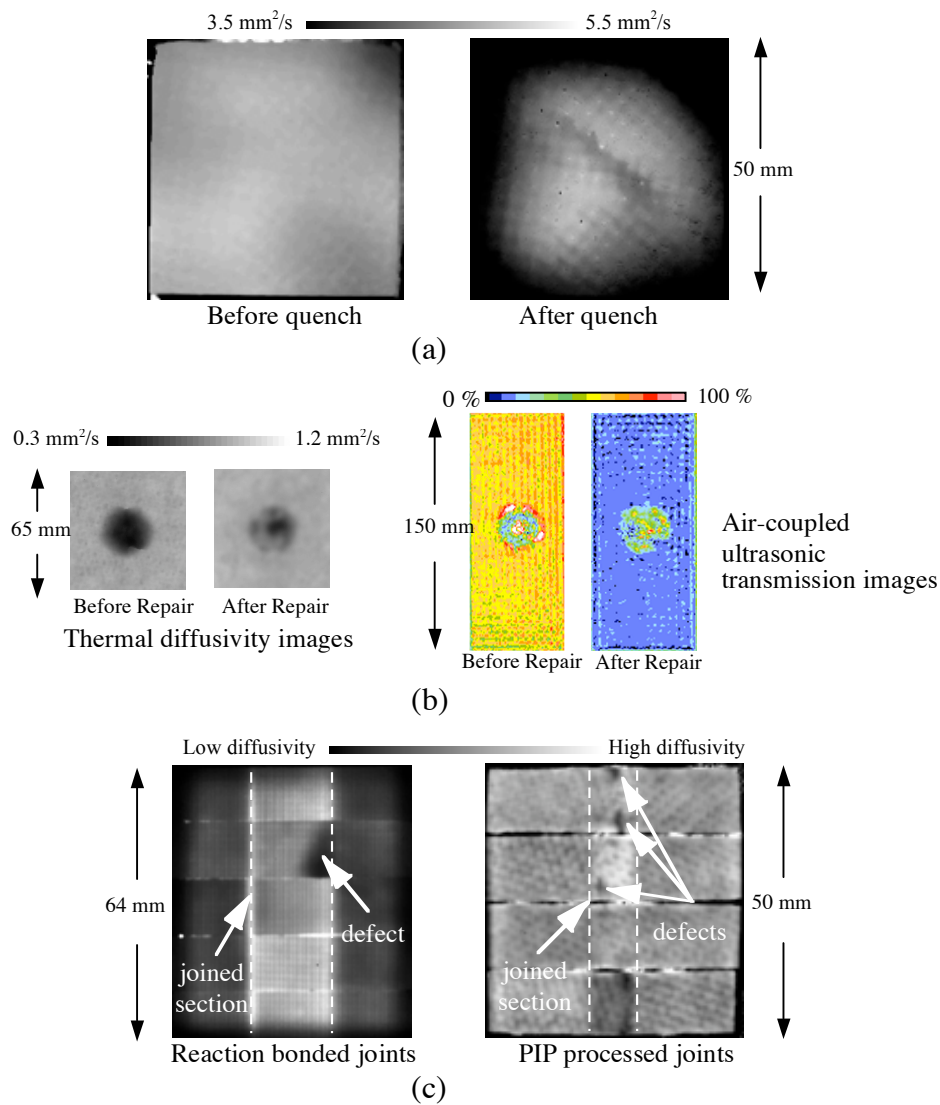

Fig. 4. (a) Thermal imaging detection of thermal shock damage; (b) thermal imaging and air-coupled ultrasonic detection of impact damage and repair; and (c) thermal imaging assessment of joint quality.

3.4   Impact damage and repair

NDE methods can detect the extent of impact damage in and assess the quality of repair provided to CMC components. Impact damage typically generates internal damage (delaminations) that may not be visible on the surface. Both impact damage and subsequent repair of SYLRAMIC^{TM} S200 CMC panels have been evaluated by two NDE methods: thermal imaging and air-coupled ultrasonics [Sun et al., 1998b]. Impact damage was introduced by using a 12.5-mm-diameter steel rod with a hemispherical head. Through-thickness air-coupled ultrasonic and thermal-diffusivity images, shown in Fig. 4b, revealed delaminations and other damage. The images of the repaired panels show significant improvement in both size and severity of the original damage. The correlation between the thermal and ultrasonic images is good.

3.5   Assessment of joint quality

The thermal imaging method has been used to characterize the quality of joints. Figure 4c shows thermal diffusivity images of CMC specimens joined by reaction-bonded SiC and by PIP processing. Several low-diffusivity regions that are likely to be defects in the joints can be observed in the joined section.

3.6   Delamination measurement

Delaminations occur mainly in 2-D cloth lay-up fiber architecture and to lesser extents in filament-wound fiber architecture. Quantification of a delamination requires determination of its size, severity, and depth [Sun, 2001]. Through-thickness thermal imaging and ultrasonic scanning methods can detect delaminations. One-sided thermal imaging and X-ray CT can be used to determine delamination depth.

Detection of delaminations was conducted on a 20.3-cm-diameter, 20.3-cm-long cylinder with a 3-mm-thick wall [Ellingson et al., 2003]. The fiber was 3M Corporation N720 cloth, laid up layer by layer, and infiltrated by the sol-gel process with an aluminosilicate matrix. Figure 5 shows the results of using both through-transmission air-coupled ultrasound and through-thickness thermal diffusivity to detect delamination. The delamination was verified by destructive sectioning, as shown in Fig. 5d. One special feature about oxides is to be noted when conducting NDE by the thermal method. Because oxide-based materials are optically translucent, one must modify the specimen surface to obtain an optically opaque surface on the thermal impulse side. On turbine engine combustors, where burn-off runs can be used, thin graphite "paints" have been successfully used.
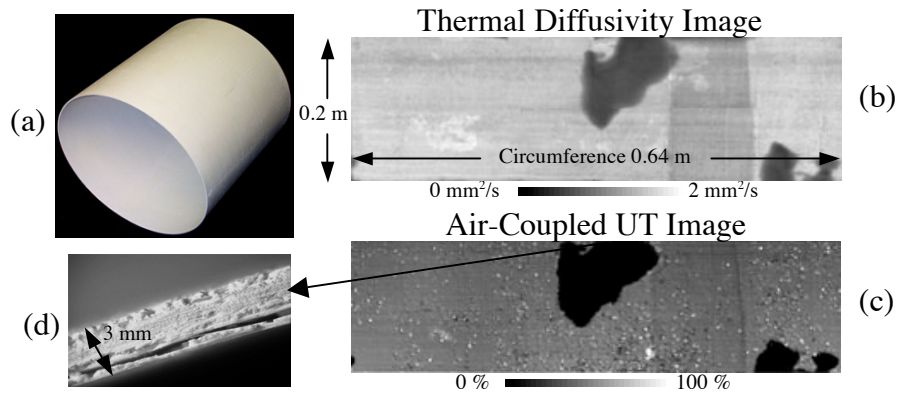
Fig. 5.   Delamination detection in oxide/oxide combustor liner. (a) Photograph of cylinder, (b) thermal diffusivity image map, (c) air-coupled ultrasound through-transmission C-scan, and (d) destructive cross-sectional image.

Measurement of delamination depth is usually calibrated by using specimens with flat-bottom holes machined at the back surface [Sun et al., 2003]. A SiC/SiC MI panel was used to determine the sensitivity and accuracy of depth detection by one-sided thermal imaging. The panel was 152 x 152 mm^2 in area and 2.6 mm in average thickness. The back surface of the plate was machined to contain 5 rows of flat-bottom holes at depths ℓ of 2.2, 1.8, 1.4, 1.0, and 0.6 mm under the front surface. Each row consisted of 8 holes with diameters d of 1, 2, 3, 4, 6, 8, 12, and 16 mm. Figure 6a, which shows the depth image predicted for the panel, indicates that the depth can only be determined for holes with a diameter-to-depth ratio larger than ≈3, although indications of the presence of smaller holes can be detected from the original thermal images. Figure 6b shows the detected depths for the 16-mm-diameter holes and nominal machining depths; the detection accuracy was good.
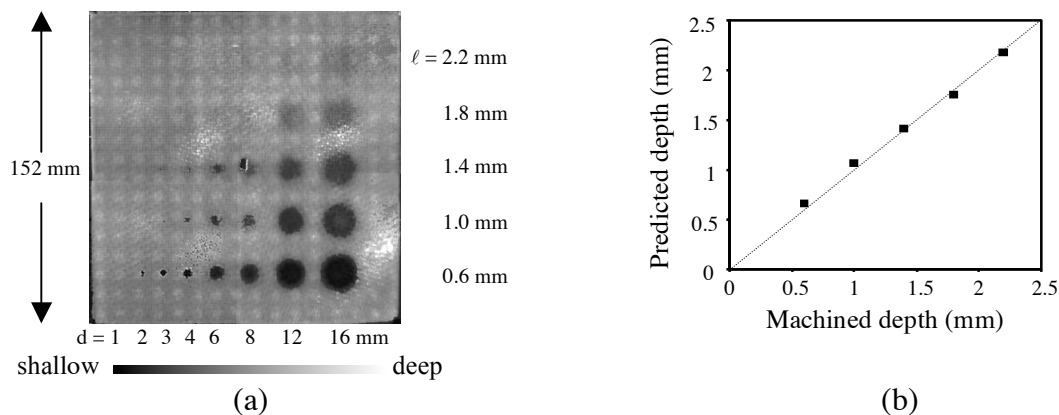

Fig. 6.   Predicted (a) depth image and (b) depth correlation for flat-bottom holes.

3.7   Detection of flaws associated with CMC/EBC material system

Reduction of oxidation-induced recession and temperature in CMC combustor liners requires the application of an environmental barrier coating (EBC) between the CMC and the hot gas. For SiC/SiC materials, current EBCs, typically 100-200 microns thick, are composed of barium-strotium-alumino-silicate (BSAS).   These EBC materials present another challenge for NDE methods. One issue to be addressed by NDE methods is assessment of uniformity and adherence of the EBC; another is detection of flaws in the CMC under the EBC. Because several processing steps are involved in fabricating a CMC/EBC liner, initial flaws within the CMC material may affect the EBC property which, in turn, will affect the liner performance.

Detection and characterization of flaws in a CMC/EBC liner was conducted at various processing stages by thermal imaging, air-coupled ultrasonics, and X-ray CT [Sun et al., 2002]. Figure 7a shows the thermal diffusivity image of the CMC liner before application of the EBC. A large delamination was found at the lower edge. To determine the delamination depth, X-ray CT and one-sided thermal imaging were performed at this region. Figure 7b shows a 0.5-mm-thick CT slice at the depth of 0.5-1 mm from the outside diameter (OD) surface, in which the defect region showed lower density. Figure 7b also shows the predicted depth from one-sided thermal imaging. The delamination depth determined by one-sided thermal imaging was ≈0.9 mm from the OD surface, which is in agreement with the CT data. Figure 7c shows the thermal diffusivity image of the CMC liner after EBC application. Expanded areas of low diffusivity were observed. This result suggests EBC dedonding, although, on the surface, the EBC appeared to be intact. This liner was subsequently installed in an operating engine. Borescope inspections of the engine at various time intervals showed that the EBC spalled off at the delamination regions that were detected by NDE. Furthermore, growth of the debonded region as a function of engine run time, shown in Fig. 7d, corresponded to the NDE data, which suggested that the EBC debonded.
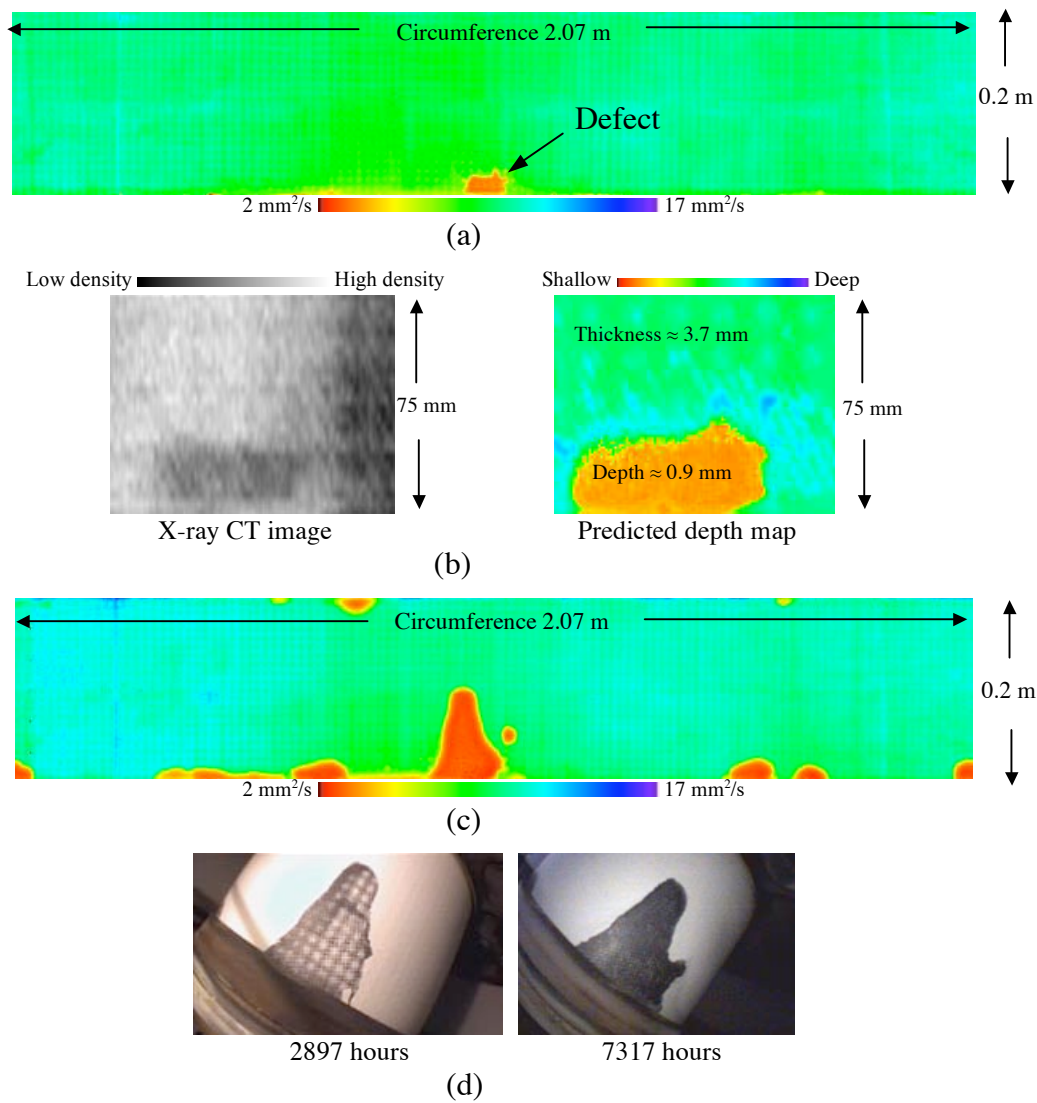
Fig. 7. NDE characterization of SiC/SiC MI combustor liner: (a) thermal diffusivity image before EBC application; (b) determination of depth of defect indicated in (a); (c) thermal diffusivity image after EBC application; and (d) EBC spallation in engine runs.

3.8 Resonant Frequency and Damping

For rotating machinery components such as bladed turbine wheels [Genge and Marsh, 1999], it is important to know the resonant frequencies and damping characteristics, because knowing the uniformity of resonant frequencies helps ensure that the structure will not go into an unstable resonant condition thereby developing a potentially catastrophic condition. Resonant frequencies and damping capacity of ceramic composites can be measured by the impact acoustic resonance NDE method. Spohnholtz [1999] and Bemis et al. [1998] have described in depth the various details involved in making these measurements.

The impact acoustic resonance test was conducted for a blisk (an integrally bladed disk) made of C/SiC [Genge and Marsh, 1999] with the setup illustrated in Fig. 1e. Figure 8a shows a photograph of the blisk under study. Figure 8b, a plot of resonant frequency for each blade before spin testing, shows that Blade 21 exhibits a significantly lower resonant frequency. Subsequent X-ray CT imaging revealed an ≈1-mm void at Blade 21.

(a)

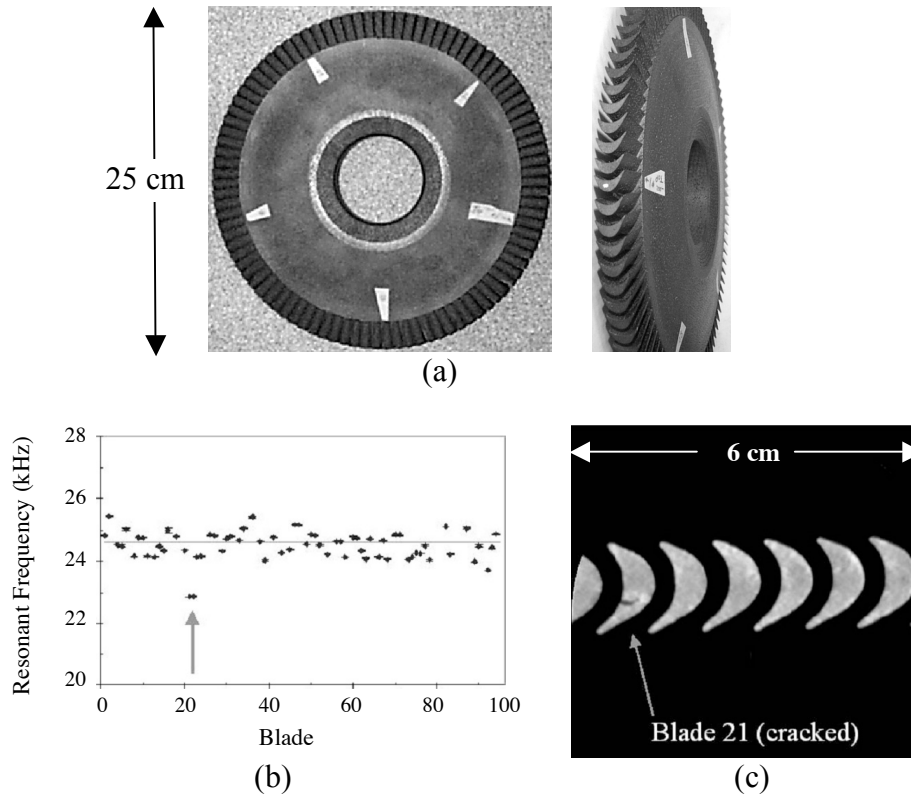
(b)   (c)

Fig. 8.   (a) Photograph of bladed disk (blisk) made of C/SiC; (b) resonant frequency of each blade of blisk; and (c) X-ray CT image showing void in Blade 21.

3.9   Health Monitoring/Remaining Useful Life

Several analytical models for life prediction of ceramic composites have been proposed [Talreja, 1989; Ahn and Curtin, 1997]. However, these models are based on micromechanics and require the constitutive properties of each component in the material (i.e., individual fibers, the matrix, and the coating on the fibers) for each condition that the material will be expected to encounter (e.g., temperature, time at load, etc.). An alternative approach is to utilize data from NDE methods that could be coupled to a more macromechanic model to predict remaining useful life, with the proviso that the component would not be subjected to conditions too far outside of certain bounds. One such approach is to measure elastic modulus of the material, which has been related to the onset and accumulation of global matrix cracking in both oxide and non-oxide CMCs [Morscher, 1999; Steel, 2000]. Figure 9 shows a typical stress-strain diagram for Hi-Nicalon/C (a SiC/C CMC) and N720/AS (an oxide/oxide material). For the SiC/C CMC, a change in the elastic modulus is noted, with the nonlinear region defining the upper limit of the

linear elastic region and the quasi-linear region. The oxide/oxide material exhibited a modulus change from onset of loading and continued to decrease until catastrophic failure.
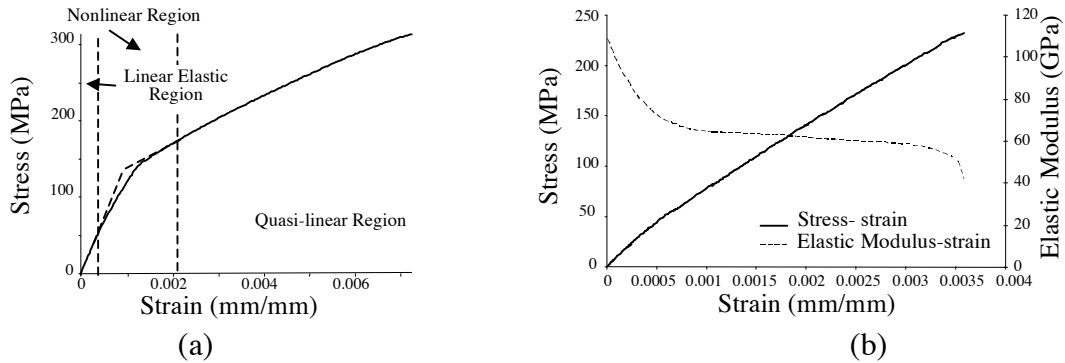

Fig. 9. Diagram of stress-strain for (a) SiC/C, showing linear elastic, nonlinear, and quasi-linear regions and (b) oxide/oxide CMC, showing continuous degradation of elastic modulus.

One method to nondestructively detect bulk changes in the elastic modulus of CMCs is from guided plate wave velocities [Chein, et al., 1994; Morscher, 1999; Deemer, 2003]. Guided plate wave velocity measurements can be directly related to in-plane elastic properties for the characterization of CMCs. Using the acousto-ultrasonic system described in Fig. 1d, we evaluated the elastic modulus degradation of SiC/C and oxide/oxide CMCs during a tensile test. Before loading, we measured an initial guided plate wave velocity. The specimen was then subjected to a series of load/unload cycles in tension. Each subsequent maximum stress load/unload cycle was 10 MPa greater than the previous cycle. At the peak stress of each cycle, the sample was held at load and the guided plate wave velocity was reacquired. The guided plate wave velocities were used to compute the damage parameter as a function of tensile stress level [Deemer, 2003]. The correlation between the damage parameters computed from the guided plate wave velocity and the secant elastic modulus determined for the stress-strain relationship was good, as seen in Figs. 10a and 10b.
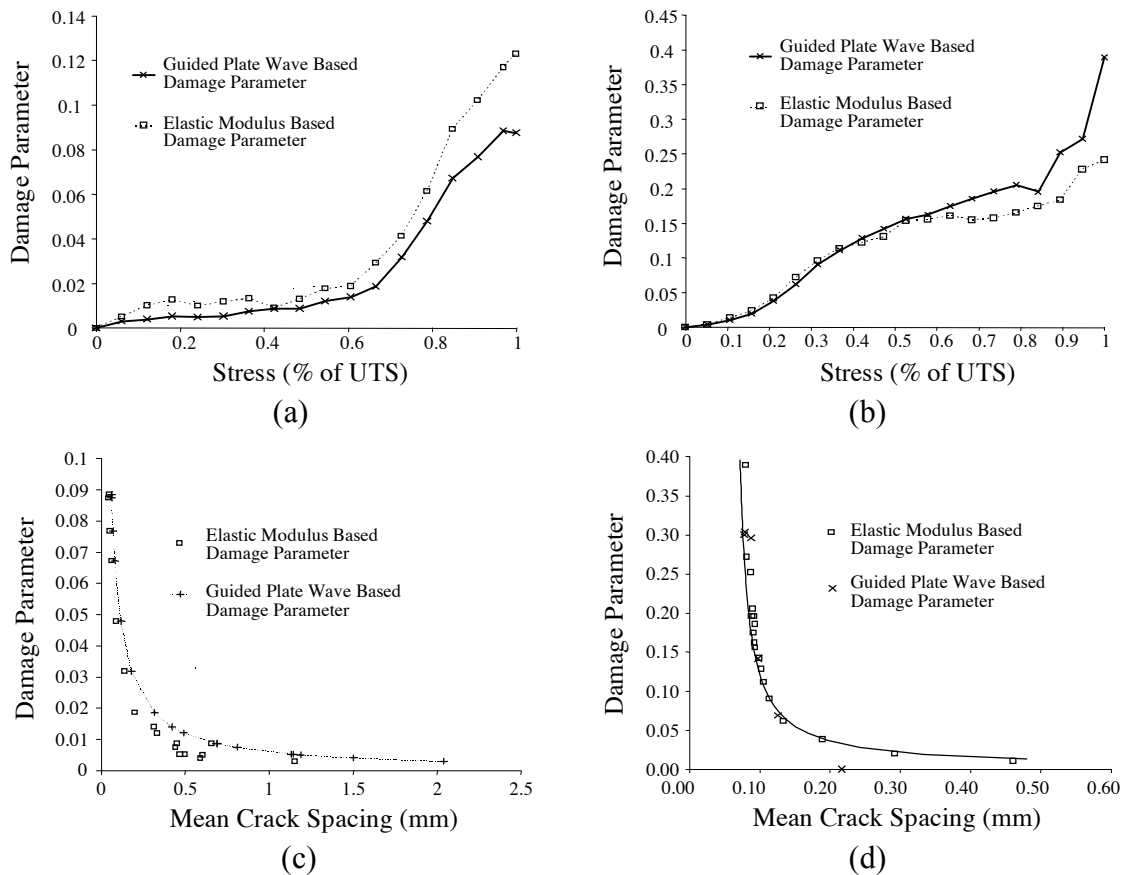
Fig. 10. Stress-damage parameter for (a) SiC/C and (b) oxide CMCs and relationship between matrix crack spacing and damage parameters for (c) SiC/C and (d) oxide CMCs computed from elastic modulus and guided plate wave velocities.

Tensile samples made from the non-oxide and oxide CMCs were used to determine the accumulation of transverse matrix cracking induced during tensile loading. Each specimen was loaded in tension to a predetermined stress. The gauge area of each monotonically loaded specimen was sectioned into 20-mm regions. The side of a 2-cm section from each specimen was polished and etched. The number of side-breaking cracks was then determined over the 20 x 3-mm region by optical photomicrography. The relationship between the average space between transverse matrix cracks and the damage parameter is shown in Figs. 10c and 10d.

4.0   Summary

CMCs are complex material systems that present unique challenges and opportunities for NDE technologies. Because multiple processing steps are involved during their fabrication, CMC components may contain large discrete defects (such as delaminations or voids) as well as many microscopic flaws such as porosities and small cracks. These flaws and defects could significantly affect the mechanical and thermal properties of CMC components. To address these challenges, five NDE methods were developed and were found to be applicable to the characterization of CMCs of various materials (oxide or non-oxide), fabricated by different

processes, and integrated with EBCs. These NDE methods include thermal imaging by both through-transmission and one-sided configurations, air-coupled ultrasonics in through-transmission mode, X-ray computed tomography, guided plate waves, and impact acoustic resonance. The NDE technologies were utilized to characterize CMC material systems during fabrication to assess process improvements and component quality. We demonstrated that these technologies are capable of detecting and characterizing defects such as porosity, delamination, and large voids in as-processed materials, as well as damage induced by impact, thermal shock, and high-temperature engine operation. In addition, initial work has been conducted to perform "health" monitoring during service and estimate "remaining" useful life of CMCs.

References

Ahn, B. K. and Curtin, W. A., 1997, "Strain and Hysteresis by Stochastic Matrix Cracking in Ceramic Matrix Composites," *J. Mech. Phys. Solids*, Vol. 45, pp. 177-209.

Bemis, R. A., Shiloh, K. and Ellingson, W. A., 1998, "Nondestructive Evaluation of Thermally Shocked Silicon Carbide by Impact Acoustic Resonance," *Trans. ASME, J. Eng. Gas Turbines and Power*, Vol. 118, pp. 491-424.

Chein, H. T., Sheen, S. H., and Raptis, A. P., 1994, "An Alternative Approach of Acousto-Ultrasonic Technique for Monitoring Material Anisotropy of Fiber-Reinforced Composites," *IEEE Trans Ultrasonics, Ferroelectrics, and Frequency Control*, Vol. 41, pp. 209-214.

Deemer, C., 2003, "Use of Plate Waves for Predicting Remaining Useful Life of Ceramic Matrix Composites," Ph. D. Dissertation, Northwestern University, Evanston, IL.

Eaton, H. E., Linsey, G., Sun, E., More, K. L., Kimmel, J., Price, J. and Miryala, N., 2001, "EBC Protection for SiC/SiC Composites in the Gas Turbine Combustion Environment: Continuing Evaluation and Refurbishment Consideration," ASME Paper 2001-GT-513.

Ellingson, W. A., Sun, J. G., More, K. L., and Hines, R. G., 2000, "Characterization of Melt-Infiltrated SiC/SiC Composite Liners Using Meso and Macro NDE Techniques," ASME Paper 2000-GT-0067.

Ellingson, W. A. and Deemer, C., 2002 "Nondestructive Evaluation Methods for CMC (defect characterization)," Department of Defense Handbook – Ceramic Matrix Composite, MIL-17-5, ed. S. T. Gonczy, pp 100-108.

Ellingson, W. A., Ikeda, Y., and Goebbels, J., 2003, Chapter 23: "Nondestructive Evaluation/Characterization," in *Ceramic Gas Turbine Component Development and Characterization*, eds., M. van Roode, M. K. Ferber, and D. W. Richerson, ASME Press, New York, pp. 493-519.

Ellingson, W. A., and Deemer, C., 2004, "Nondestructive Evaluation of Structural Ceramics," *Handbook of Advanced Materials*, ed. J. K. Wessel, McGraw-Hill, Hoboken, NJ.

Evans, A. G. and Naslain, R., 1995a, "High-Temperature Ceramic-Matrix Composites I: Design, Durability and Performance," *Ceram. Trans.* Vol. 57, Am. Ceram. Soc.

Evans, A. G. and Naslain, R., 1995b, "High-Temperature Ceramic-Matrix Composites II: Manufacturing and Materials Development," *Ceram. Trans.* Vol. 58, Am. Ceram. Soc.

Genge, G. G. and Marsh, M. W., 1999, "Carbon Fiber Reinforced/Silicon Carbide Turbine Blisk Testing in the SIMPLEX Pump," *Proc. of the 49th Joint Army, Navy, Air Force (JANNAF) Meeting*, pp. 89-97.

Ko, F. K., 1989, "Preform Fiber Architecture for Ceramic-Matrix Composites," *Am. Ceram. Bulletin*, Vol. 68, No. 2, pp. 401-414.

Krajcinovic, D., 1984, "Continuum Damage Mechanics," *Appl. Mech. Rev.*, Vol. 37, No. 1, pp. 1-6.

Miriyala, N., Fahme, A., and van Roode, M., 2001, "Ceramic Stationary Gas Turbine Program - Combustor Liner Development Summary," ASME Paper 2001-GT-512, presented at the International Gas Turbine and Aeroengine Congress and Exposition, New Orleans, Louisiana, USA, June 2001.

Morscher, G. N., 1999, "Modal acoustic Emission of Damage Accumulation in a Woven SiC/SiC Composite," *Composite Sci. Technol.*, Vol. 59, pp. 687-97.

Parker, W.J., Jenkins, R.J., Butler, C.P., and Abbott, G.L., 1961, "Flash Method of Determining Thermal Diffusivity, Heat Capacity, and Thermal Conductivity," *J. Appl. Phys.*, Vol. 32, pp. 1679-1684.

Pillai, T. A. K., Ellingson, W. A., Sun, J. G., Easler, T. E., and Szweda, A., 1997, "A Correlation of Air-Coupled Ultrasonic and Thermal Diffusivity Data for CFCC Materials," in *Ceram. Eng. Sci. Proc.*, Vol. 18, No. 4, pp. 251-258.

Price, J., Jimenez, O., Parthasarthy, V. J., Miryala, N. and Levoux, D., 2000, "Ceramic Stationary Gas Turbine Development Program: Seventh Annual Summary: ASME Paper 2000-GT-75.

Spohnholtz, T. W., 1999, "Development of Impact Resonant Spectroscopy for Characterizing Structural Ceramic Components," M.S. Thesis, University of Illinois-Chicago, 1999.

Steel, S. G., 2000, "Monotonic and Fatigue Loading Behavior of an Oxide/Oxide Ceramic-Matrix Composite," M.S. Thesis, Air Force Institute of Technology, Wright-Patterson Air Force Base, OH.

Stuckey, J., Sun, J. G., and Ellingson, W. A., 1998, "Rapid Infrared Characterization of Thermal Diffusivity in Continuous Fiber Ceramic Composite Components," in *Nondestructive Characterization of Materials VIII*, ed. R. E. Green Jr., Plenum Press, New York, pp. 805-810.

Sun, J. G., Easler, T. E., Szweda, A., Pillai, T. A. K., Deemer, C. and Ellingson, W. A., 1998a, "Thermal Imaging and Air-Coupled Ultrasound Characterization of a Continuous Fiber Ceramic Composite," in *Ceramic Eng. Sci. Proc.*, Vol. 19, Issue 3, pp. 533-540.

Sun, J. G., Petrak, D. R., Pillai, T. A. K., Deemer, C. and Ellingson, W. A., 1998b, "Nondestructive Evaluation and Characterization of Damage and Repair for Continuous Fiber Ceramic Composite Panels," in *Ceram. Eng. Sci. Proc.*, Vol. 19, Issue 3, pp. 615-622.

Sun, J. G., Deemer, C., Ellingson, W. A., Easler, T. E., Szweda, A., and Craig, P. A., 1999, "Thermal Imaging Measurement and Correlation of Thermal Diffusivity in Continuous Fiber Ceramic Composites," in *Thermal Conductivity 24*, eds. P. S. Gaal and D. E. Apostolescu, pp. 616-622.

Sun, J. G., 2001, "Analysis of Quantitative Measurement of Defect by Pulsed Thermal Imaging," in *Review of Quantitative Nondestructive Evaluation*, Vol. 21, ed. D.O. Thompson and D.E. Chimenti, pp. 572-576.

Sun, J. G., Erdman, S., Russel, R., Deemer, C., Ellingson, W. A., Miriyala, N., Kimmel, J. B., and Price, J. R., 2002, "Nondestructive Evaluation of Defects and Operating Damage in CFCC Combustor Liners," in *Ceram. Eng. Sci. Proc.*, Vol. 24, Issue 3, ed. H-T Lin and M. Singh, pp. 563-569.

Sun, J. G., 2003, "Method for Determining Defect Depth Using Thermal Imaging," U.S. Patent No. 6,542,849, issued April 2003.

Sun, J. G., Erdman, S., and Connolly, L. 2003, "Measurement of Delamination Size and Depth in Ceramic Matrix Composites Using Pulsed Thermal Imaging," in *Ceram. Eng. Sci. Proc.*, Vol. 24, Issue 4, ed. W. M. Kriven and H-T Lin, pp. 201-206.

Talreja, R., 1989, "Damage Development in Composites: Mechanisms and Modeling," *J. Strain Anal.*, Vol. 24, No. 4, pp.215-22.

Wang, Y. L., Webb, J. E., Singh, R. N., Sun, J. G., and W. A. Ellingson, 1998, "Evaluation of Thermal Shock Damage in 2-D Nicalon^{TM} Al$_2$O$_3$ Woven Composite by NDE Techniques," in *Ceram. Eng. Sci. Proc.*, Vol. 19, Issue 3, pp. 607-614.